Nanoscale

Accepted Manuscript

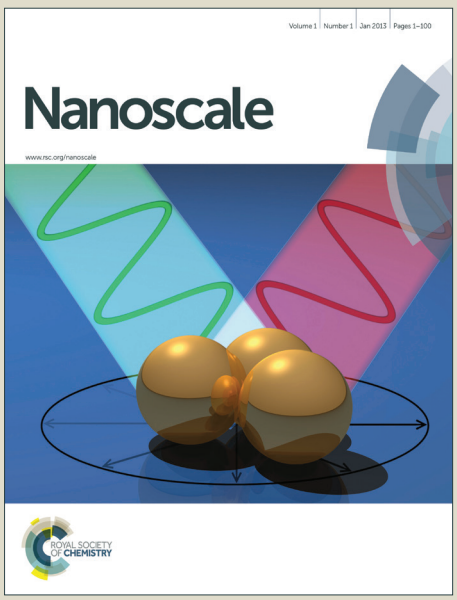

ROYAL SOCIETY OF CHEMISTRY

www.rsc.org/nanoscale

Journal Name

RSCPublishing

ARTICLE

Fabrication of Flexible, Transparent and Conductive Films from Single-walled Carbon Nanotubes with High Aspect Ratio Using *Poly*(((furfuryl methacrylate)-*co*-(2-(dimethylamino)ethyl methacrylate)) as a New Polymeric Dispersant

Cite this: DOI: 10.1039/x0xx00000x

Received 00th January 2012,
Accepted 00th January 2012

DOI: 10.1039/x0xx00000x

www.rsc.org/

Taeheon Lee,[a] Byunghee Kim,[a] Sumin Kim,[b] Jong Hun Han,[c] Heung Bae Jeon,[d] Young Sil Lee,[e*] Hyun-jong Paik[a,b*]

We synthesized *poly*((2-dimethylamino)ethyl methacrylate-*co*-furfuryl methacrylate) (*p*(DMAEMA-*co*-FMA)) for dispersion of single-walled carbon nanotubes (SWCNTs) and maintained their high aspect ratios. The nanotubes' length and height were 2.0 μm and 2 nm, as determined by transmission electron microscopy and atomic force microscopy, respectively. Transparent conductive films (TCFs) were fabricated by individually dispersed long SWCNTs onto a flexible polyethylene terephthalate substrate. The sheet resistance (R_s) was 210 Ω/□ with 81% transmittance at a wavelength of 550 nm. To reduce their R_s, the TCFs were treated with HNO_3 and $SOCl_2$. After treatment, the TCFs had an R_s of 85.75 Ω/□ at a transmittance of 85%. The TCFs exhibited no appreciable change over 200 repeated bending cycles. Dispersing SWCNTs with this newly synthesized polymer is an effective way to fabricate a transparent, highly conductive and flexible film.

1. Introduction

Since the invention of carbon nanotubes (CNTs),[1] they have been studied with great interest and applied in various fields due to their unique electrical[2-15] and mechanical properties.[16-18] In particular, single-walled carbon nanotubes (SWCNTs), which have remarkable electrical mobility, conductivity[19] and work functions,[20] are considered promising in electrical applications such as transistors,[21-23] sensors,[24-26] memory devices[27, 28] and conducting films.[6-17, 29-32] SWCNT transparent conductive films (TCFs) are thought to have a great deal of promise for electrical applications such as replacing indium tin oxide (ITO) in touch panels due to their light weight and flexibility.[15, 16, 33-37] SWCNTs are very promising as components of the patterned TCFs used in capacitive touch panels because of their chemical and environmental stability coupled with low pattern recognition, while conducting polymers and nanowires have low stability and high pattern recognition.

CNTs exist as bundles due to strong π–π stacking[38] and their dispersion is a major challenge that has been investigated in the last decades. To overcome these issues, it is important to disperse CNTs without introducing any additional defects into their crystalline structure by, for example, damaging their intratubes or chopping them and to establish good contact between individual CNTs. Hence, the dispersion of CNTs is

addressed largely by two different types of methods: covalent and non-covalent. Although CNT dispersion using covalent methods is efficient, it can reduce their conductivity by affecting the intrinsic structures of the CNTs,[39] while non-covalently-dispersed CNTs retain their properties with limited defects.[6, 14, 35, 40, 41] However, the non-covalent functionalization of CNTs has some drawbacks, including the difficulty of maintaining the intrinsic aspect ratio because the CNTs shorten during the dispersion process.[42-44] For example, small molecular dispersants such as sodium dodecyl sulfonate (SDS) and sodium dodecylbenzensulfonate (SDBS) widely used to disperse CNTs demand high-power ultrasonication, which reduces the length of the original CNTs from several micrometers to less than 1 μm.[45-47] This shortened length can reduce the CNTs' electrical, optical and mechanical properties. The reduction in the CNTs' electrical properties increases the contact resistance of CNT networks, creating a bottleneck in the real application of CNT-coated conductive films. The percolation threshold of CNTs on the electrical conductivity of TCFs scales inversely with the aspect ratio of the CNTs.[48] Thus, the transmittance of a TCF using CNTs can be enhanced by the low percolation threshold of the CNTs. In addition, the CNTs' aspect ratio reduces the network between the CNTs, which can improve the stability of the electrical conductivity when the TCF is deformed (i.e., bent or tilted), making its application more flexible. Although this CNT dispersion technique has been developed based on a great deal of research, CNTs still need to be dispersed more effectively. Polymeric dispersants reduce the entropy penalty function and prevent the aggregation of SWCNTs more effectively under mild conditions.[49]

In our previous study,[35] we fabricated CNT-coated TCFs using *poly*((styrene-*co*-(2-dimethylamino)ethyl methacrylate)) (*p*(St-*co*-DMAEMA)) as the polymeric dispersant. This polymer dispersed the CNTs effectively without significantly shortening them.

To further enhance the electrical conductivity of the CNT-based TCF, we have synthesized and employed a new polymer dispersant, *poly*(((furfuryl methacrylate)-*co*-(2-(dimethylamino)ethyl methacrylate)) (*p*(FMA-*co*-DMAEMA)). These polymers could be used to disperse SWCNTs with high aspect ratios (length approximately 2.0 μm) and without significant defects. TCFs were prepared using a well-dispersed SWCNT solution on a polyethylene terephthalate (PET) substrate, followed by chemical treatment with HNO_3 and $SOCl_2$. After treatment, the TCFs showed a reduction of sheet resistance (R_s) from 210 Ω/□ (81% transmittance at 550 nm) to 85.75 Ω/□ (85% transmittance) caused by removing any residue. The dispersion stability and quality of the SWCNT dispersion were characterized using a dispersion stability analyzer and a transmission electron microscope (TEM). The data revealed that the SWCNTs dispersed using our new copolymers were longer than those of the previous studies by a factor of 1.5. The height of the exfoliated SWCNTs was measured using an atomic force microscope (AFM) and the defects on the SWCNT structures were studied using a Raman spectroscope. The surfaces of SWCNT-coated TCFs were investigated using a scanning electron microscope (SEM). The transmittance and R_s of the TCFs were determined by UV-visible spectroscopy and four-point probe resistance measurements, respectively.

2. Experimental

2.1 Materials

SWCNTs (1.0–1.2 nm in diameter, 5–20 μm in length) made by arc-discharge method were purchased from Nano Solution Co., Ltd. (Korea). 2-(dimethylamino)ethyl methacrylate (DMAEMA, 98%, Sigma-Aldrich) was purified before use by passing it through an alumina column to remove inhibitors. Copper(I) bromide (CuBr, 99%, Sigma-Aldrich) was purified according to the reported procedure [50]. Tertrahydrofuran (THF, 99.8%, J.T. Baker), 4,4′-Dinonyl-2,2′-dipyridyl (dNbpy, 97%,Sigma-Aldrich), ethyl 2-bromoisobutyrate (EBiB, 99%,Sigma-Aldrich), furfural (98.0%, TCI Chemicals), and sodium borohydride (NaBH4, 95%, TCI Chemicals) were used as-received.

2.2 Synthesis of furfuryl alcohol

Sodium borohydride (3.8 g, 100 mmol) was added dropwise to a solution of furfural (19.2 g, 200 mmol) in methanol (100 mL) at 0 °C under an N_2 atmosphere. The resulting mixture was stirred for 2 h at room temperature. Next, the solvent was evaporated, and the residue was dissolved in ether. The organic layer was washed with water, and the aqueous layer was extracted with ether twice. The combined organic layer was dried over $MgSO_4$. The filtrate was distilled at 70 °C to produce a clear oil of furfuryl alcohol (FA) (14.5 g, 74%). ^{1}H NMR (500 MHz, CDCl3, ppm): δ = 7.40 (s, 1 H), 6.34 (d, 1 H), 6.29 (d, 1 H), 4.61 (s, 2 H).

2.3 Synthesis of furfuryl methacrylate

Furfuryl alcohol (FA) (10 g, 101.9 mmol), triethylamine (30.94 g, 305.7 mmol) and dichloromethane (100mL) were added to a 250 mL round-bottomed flask at 0°C under a nitrogen atmosphere. Methacryloyl chloride (15.98 g, 152.9 mmol) was added dropwise over a period of 10 min. The reaction was carried out while stirring for 2 h as the mixture slowly came to room temperature. The precipitate was removed, and the filtrate was washed with a saturated NaCl aqueous solution, dried over MgSO4, filtered, and concentrated. The resulting residue was purified by vacuum distillation at 75 ^{o}C (6.77 g, 40%). ^{1}H NMR (CDCl3, ppm): δ = 7.42 (s, 1 H), 6.42 (d, 1 H), 6.36 (m, 1 H), 6.13 (s 1 H), 5.57 (s, 1 H), 5.14 (s, 2 H), 1.95 (s 3 H).

2.4 Synthesis of *p*(DMAEMA-*co*-FMA)

P(FMA-*co*-DMAEMA) was synthesized using atom transfer radical polymerization (ATRP) from DMAEMA and FMA. CuBr/dNbpy was used as a catalyst, and EBiB was used as an initiator. DMAEMA (0.511 mL, 3.03 mmol), FMA (1.09 mL,

7.07 mmol), dNbpy (55.1 mg, 0.134 mmol), and anisole (1.50 mL) were added to a 5 mL Schlenk flask. The mixture in the flask was degassed three times via a freeze–pump–thaw cycle. After degassing, the flask was filled with nitrogen, and CuBr (9.67 mg, 6.74 × 10–2 mmol) was quickly added to the frozen mixture. The flask was sealed with a glass stopper, and then evacuated and backfilled with nitrogen three times before the initiator, EBiB (10 μL, 6.74 × 10–2 mmol) was added. The mixture was stirred for 90 min at 70 °C under an N_2 atmosphere, then diluted with THF and passed through a neutral alumina column to remove the copper catalyst. After column separation, the *p*(FMA-*co*-DMAEMA) was isolated after in hexane and dried under vacuum at room temperature for 24 h (0.770 g, 46.7%). This method was used to prepare other polymers of FMA and DMAEMA with monomer ratios of 0:100, 30:70, 50:50, 70:30, and 100:0.

2.5 Dispersion of SWCNTs

The *p*(FMA-*co*-DMAEMA) (20.0 mg) was dissolved in THF (20.0 mL), The SWCNTs (2.0 mg) were added to this polymer solution and dispersed by sonication in a bath-type sonicator (WUC-D22H, DAIHAN Scientific Co. 40kHz, 200 Watt) for 3 h. The dispersed SWCNT solution was centrifuged at 10000 rpm for 10 min to remove both bundled SWCNTs and the metal catalyst [51]. The well-dispersed SWCNT solution was obtained from the supernatant.

2.6 Fabrication of transparent conductive films

The SWCNT-coated transparent conductive films were prepared by spin-coating the purified SWCNT solution on a poly(ethylene terephthalate) (PET) substrate. Using a syringe pump, 2.5 mL of the dispersed-SWCNT solution was deposited on a substrate film (25 mm × 25 mm) at a constant rate of 2500 rpm for 15 min. After spin coating, the films were washed with THF to remove any residual polymers and then dried in a vacuum oven. To reduce the R_s value of the TCFs, each films was immersed in 12 M HNO_3 for 1 h and in $SOCl_2$ for 1 h. Next, the films were washed with THF and dried under vacuum.

2.7 Characterization

The number average molecular weight (M_n) and molecular weight distribution (M_w/M_n) were determined using gel permeation chromatography (GPC) calibrated with *poly*(methyl methacrylate) (PMMA) standards. The chromatograph was equipped with an Agilent 1100 pump, a RID detector, and PSS SDV (5 μm; 105, 103, 102 Å; 8.0 × 300.0 mm) columns. ^{1}H NMR spectra were obtained using a 500 MHz Agilent Superconducting FT-NMR spectrometer with chloroform-d as the solvent. The structural characteristics of the SWCNT sheets were investigated using an NTEGRA Spectra confocal Raman spectrometer (NT-MDT) with an excitation wavelength of 532 nm. The de-bundled SWCNTs in the dispersion solution were characterized using transmission electron microscopy (with an H-7600 TEM from Hitachi) and atomic force microscopy (AFM). Droplets of the solution were applied directly to carbon-coated copper grids. Non-contact (tapping) AFM was performed with an n-tracer SPM (Nanofocus). The cantilever was made of silicon and had a resonant frequency of approximately 320 kHz and a nominal radius of curvature of less than 8 nm. Images were obtained at room temperature in air. The dispersion stabilities of the SWCNTs in THF were determined using a Turbiscan LAB dispersion stability analyzer (Formulaction). The transmittance profiles obtained from the dispersion stability analyzer were assessed as a function of time (7 selected scans for 3 days) and of sample height (5–30 mm). The network structures of the SWCNT films were observed using an S-4800 field emission scanning electron microscope (FE-SEM, Hitachi). The transmittances and sheet resistances of the TCFs were measured using an OPTIZEN 3220UV UV-vis spectrophotometer (MECASYS Co.) at 550 nm and a CMT-SR1000N four-point probe measurement (A.I.T.), respectively. The flexibility and durability of the SWCNT-based TCFs were estimated by measuring the change in resistance using a computer system with a digital multimeter (Agilient 34401A) during the cyclic bending test. The cyclic test was performed on rectangular TCF samples. The tests were carried out using a home-made fatigue machine at 2 Hz while maintaining a constant linear vertical movement with a 7 mm stroke. A cyclic bending stress was applied to the films dynamically using a moving jig.

3. Results and discussion

3.1 Synthesis of monomer and polymeric dispersant

The FMA was synthesized from the reduction of furfural and their subsequent coupling with methacryloyl chloride. The structure of the FMA was confirmed from ^{1}H NMR, as shown in Figure 1. The FMA and DMAEMA were polymerized in different ratio by ATRP to wield series of *p*(FMA-*co*-DMAEMA)s (Scheme 1). The FMA in the *p*(FMA-*co*-DMAEMA) was expected to act as the anchoring group while DMAEMA was expected to as the stabilizer. The chemical structure of *p*(FMA-*co*-DMAEMA) was characterized using ^{1}H NMR spectroscopy in Figure 2. The ratio of methylene proton peak integrations in FMA (at δ = 4.92 ppm) and DMAEMA (at δ = 4.02 ppm) were in agreement with their conversion ratio directly calculated from GC considering the minor differentiation in the values was within allowed error. The resonance of protons was assigned as shown in Figure 2. The molar composition was confirmed to be 70:30 (FMA:DMAEMA) by comparing the integral area for the methylene (-$CO_2C\mathbf{H}_2$-) of the FMA and DMAEMA units at δ = 4.92 ppm and 4.02 ppm of protons, respectively. The composition, molecular weight, and polydispersity index for each polymer dispersant are listed in Table 1.

Figure 1

Scheme 1

Table 1

Figure 2

3.2 Characterization of the SWCNT dispersions

The polymeric dispersant content, which could be an impurity, was less than that previously reported. After sonication, the SWCNT dispersion with *p*(FMA-*co*-DMAEMA) appeared as a dark solution and maintained its dispersion for up to 1 month without significant sedimentation of the SWCNT. The dispersion stability of the SWCNT solutions with polymeric dispersants over 3 days is shown in Figure 3. SWCNTs in solution with both homopolymers (dispersants **1** and **5**) aggregated and separated as a result of rebundling, which resulted in an enhancement of the transmittance values over time. The increments in transmittance after three days were 21.2 and 4.98 for dispersants **1**, and **5**, respectively. And dispersant 4 showed phase separation quickly. In contrast, the SWCNT solution with the copolymer, dispersant **2 and 3**, was well-dispersed and its transmittance values increased only slightly to,1.39 and 0.1, respectively. From these results, it was determined that SWCNT solutions were homogeneously well-dispersed in solution of copolymers having appropriate composition window than the other dispersants.

Figure 3

These results were further confirmed by the presence of individual SWCNTs in the dispersion, as observed by TEM. Figure 4(a) shows the TEM images of the SWCNTs with dispersant 2 and the distribution of SWCNT lengths is shown in Figure 4(b). The lengths of individual SWCNTs were between several hundred nanometers and a few micrometers with an average of 2.0 (±0.74) μm. This is twice more the length previously reported for individually-suspended HiPco SWCNTs obtained using sodium dodecylbenzene sulfonate (SDBS), which is considered one of the best surfactants for dispersing SWCNTs in an aqueous solution.[47]

Figure 4

Furthermore, the average length of the individual SWCNTs was greater than the length (1.35 μm) reported using the same type of SWCNTs produced by the arc-discharge method and dispersed in an organic solvent (N-methyl-2-pyrrolidone) under optimal sonication conditions.[52] It is worth mentioning that more than 96% of the SWCNTs were longer than 1 μm. Individually-separated SWCNTs were found in the AFM image shown in Figure 5(a-b). The height profile of the exfoliated SWCNTs is shown in Figure 5(c). It is clear that the SWCNTs were individually dispersed and maintained their high aspect ratios. It is important to maintain a high aspect ratio after dispersion because the length of the SWCNTs influences the electrical properties of the resulting SWCNT network. This makes for a smaller number of junctions between SWCNTs in the network, lowering the contact resistance.[37, 53] According to these dispersion stability, TEM and AFM results, *p*(FMA-*co*-DMAEMA) performed well in dispersing SWCNTs and the SWCNT solution was suitable for producing well-dispersed SWCNTs for use in TCFs.

Figure 5

3.3 Characterization of the TCFs

The TCFs were fabricated by spin-coating onto flexible PET substrates using the SWCNTs dispersed solution with polymeric dispersants. The R_s of the TCFs fabricated using copolymer dispersant 2 and 3 exhibited 210 Ω/□ (at 80% transmittance) and 359 Ω/□ (at 83% transmittance), respectively, without any further treatment as shown in figure 6. Their average R_s values correlate with the transmittance of TCFs made with various amounts of SWCNT solution. To further reduce their R_s values, the films with dispersant 2 were immersed in HNO_3 and $SOCl_2$. After this chemical treatment, the value of R_s was significantly reduced to 85.75 Ω/□ at 85% transmittance. This reduction in the value of R_s is a considerable achievement when compared with the results of previous research.[7-11, 13, 14, 29, 54] The chemical treatment with HNO_3 and $SOCl_2$ provides not only a means of removing the residual impurities but also a densification of the SWCNT network and p-type doping of the SWCNTs. This result is consistent with previous work.[7, 9, 10, 15, 55] Furthermore conductivity stability of treated TCFs almost didn't changed for 7 days.

Figure 6

Transmittance and R_s are the most important parameters for TCFs, and R_s is sensitive to the value of the transmittance. The R_s is indirectly proportional to the transmittance. The ratio of the direct current conductivity (σ_{dc}) to the optical conductivity (σ_{op}) was calculated using the Figure of Merit (FOM) equation:

$$T(\lambda) = \left(1 + \frac{Z_0}{2R_0}\frac{\sigma_{op}}{\sigma_{dc}}\right)^{-2}, \quad \text{Equation (1)}$$

where Z_0 is the impedance of free space (377 Ω) and T(λ) is the wavelength-dependent transmittance. σ_{dc} / σ_{op} is directly related to R_s and the transmittance. The values of R_s and T can be substituted into Equation 1 to find σ_{dc} / σ_{op}. As shown in table 2, before acid treatment, the value of FOM was 7.6; after treatment with HNO_3, the value increased to 16.1. Furthermore, the FOM increased to 26.0 after treatment with $SOCl_2$. The electrical conductivity of the treated TCF increased up to 3.4 times compared with the untreated TCF. The FOM value of 26.0 was higher than the previous reported value of 17 after

HNO_3 and $SOCl_2$.[7] This value is much higher than the minimum requirement for TCFs used in flat panel displays.

Table 2

The surface morphology of the TCFs was investigated using FE-SEM. The formation of an SWCNT network from well-dispersed SWCNTs is shown in Figure 7(a). Impurities due to residue were observed on the surface. Although the TCFs were prepared using dispersed SWCNTs with high aspect ratios, residual polymer and polymer wrapping SWCNTs could function as insulators, reducing the conductivity. However, after treatment, only a few impurities could be observed on the TCFs' surfaces, as shown in Figure 7(b). It was not surprising that the thickness of the SWCNT film was reduced when the polymeric dispersant was removed or that the number of vacancies between SWCNTs in the network was enhanced. These results indicate that the residual polymeric dispersant on the surface was removed by the chemical treatment. The reduction in the thickness of the SWCNTs revealed that the polymer covered the side walls and tube-tube junctions of the SWCNTs before the chemical treatment. As a result, the chemically treated TCFs had not only improved electrical conductivity but also enhanced transmittance.

Figure 7

Another critical issue with the acid treatment of SWCNT surfaces is that defects in the nanotubes will be introduced. The number of defects in the SWCNTs was calculated based on the Raman spectra shown in Figure 8. Figure 8(a) shows the Raman spectra of pristine, coated, and chemically treated SWCNTs. After acid treatment, the G-band was blue shifted, indicating p-doping[56], which results in an electron being transferred from an SWCNT to an absorbed dopant (HNO_3 or $SOCl_2$) An appreciable peak shift in the D-band was observed when the pristine SWCNTs were compared with the SWCNT coatings and the chemically treated SWCNT films. A peak at ~2700 cm^{-1}, corresponding to the G' band in crystalline CNT, appeared as an overtone of the D band with a frequency twice that of the D-band.[57] As shown in Figure 8(b), the intensity of the D-band was proportional to the intensity of the G'-band. (The value for pristine SWCNT deviated slightly from the master line because this sample was a powder instead of a coating on a PET film.) Recently, it has been reported that this change in the G' band could be seen as evidence for p- and n-type doping in the SWCNTs[58]. Thus, chemically treating the SWCNT TCFs increased the relative intensities of the D and G' bands, increased the number of defects and amount of p-type doping on the SWCNT surfaces and contributed to the removal of the residual copolymers. The Raman spectra revealed few defects after chemical treatment.

Figure 8

The ratio of induced disorder (I_D) to in-plane vibration (I_G) in the Raman spectra indicates the degree of defectiveness of the SWCNTs. After chemical treatment, the value of I_D/I_G was slightly different. It changed from 4.0% (SWCNT-coated film) to 5.0% (HNO_3-treated film) and to 8.3% ($SOCl_2$-treated film); these values are listed in Table 3.

Table 3

The mechanical stability of the TCFs was investigated for applications such as touch panels. The R_s values were measured after a given number of bending cycles. The films were bent 200 times and R_s was measured every 5 bending cycles. As shown in Figure 7, there was no significant increase in R_s after 200 bending cycles. An increase of less than 10% in the R_s value of SWCNT TCF was observed after 200 bending cycles. This is mainly because a small number of network junctions with a high aspect ratio of SWCNTs were present after the SWCNTs were dispersed by the newly-synthesized polymer. This confirms the outstanding flexibility and durability of TCFs.

Figure 9

Conclusions

SWCNT has attracted considerable interest as a material with applications in electrical fields. However, one prominent issue is how to disperse bundled SWCNTs with high aspect ratios without introducing extra defects. We synthesized a new polymer, *p*(FMA-*co*-DMAEMA), for use as a polymeric dispersant of SWCNTs. The SWCNT/*p*(FMA-*co*-DMAEMA) solution exhibited good dispersity and particle stability determined by number of characterization techniques. According to these results, SWCNTs could be homogeneously well-dispersed with high aspect ratio in solution with *p*(FMA-*co*-DMAEMA) and hence, was suitable for use in TCFs. TCFs fabricated from dispersed SWCNTs had low sheet resistance (210 Ω/□) and high transmittance (81% at 550 nm). To remove residual polymers, the TCF films were chemically treated using HNO_3 and $SOCl_2$. As a result of this treatment, R_s decreased significantly to 85.75 Ω/□ at 85% transmittance, a reduction of 40%. Furthermore, the TCFs were very durable; retained their low resistance after 200 bending cycles.

Acknowledgements

This work was supported by the Active Polymer Center for Pattern Integration (No. R11-2007-0056091) and Basic Science Research Program through the National Research Foundation of Korea (NRF) grant funded by the Korea government (MSIP) (2013R1A2A2A01068818) and the Industrial Strategic Technology Development Program (10045051) funded by the Ministry of Trade, Industry and Energy (MOTIE) of Korea.

Notes and references

[a] Department of Polymer Science and Engineering, Pusan National University, 2, Busandaehak-ro 63beon-gil, Geumjeong-gu, Busan 609-735, Korea

[b] Department of Advanced Circuit Interconnection, Pusan National University, San 30 2, Busandaehak-ro 63beon-gil, Geumjeong-gu, Busan 609-735, Korea

[c] School of Applied Chemical Engineering, Chongnam National University, 77 Yongbong-ro, Buk-gu, Gwangju 500-757, Korea

[d] Department of Chemistry, Kwangwoon University, 20, Gwangun-ro, Nowon-gu, Seoul 139-701, Korea

[e] ICT Convergence Research Center, Kumoh National Institute of Technology, 1 Yangho-dong, Gumi, Gyeongbuk 730-701, Korea

1. S. Iijima, *Nature*, 1991, **354**, 56-58.
2. R. S. Ruoff and D. C. Lorents, *Carbon*, 1995, **33**, 925-930.
3. M. M. J. Treacy, T. W. Ebbesen and J. M. Gibson, *Nature*, 1996, **381**, 678-680.
4. R. H. Baughman, A. A. Zakhidov and W. A. de Heer, *Science*, 2002, **297**, 787-792.
5. S. J. Tans, M. H. Devoret, H. Dai, A. Thess, R. E. Smalley, L. J. Geerligs and C. Dekker, *Nature*, 1997, **386**, 474-477.
6. B. Dan, G. C. Irvin and M. Pasquali, *ACS Nano*, 2009, **3**, 835-843.
7. J. W. Jo, J. W. Jung, J. U. Lee and W. H. Jo, *ACS Nano*, 2010, **4**, 5382-5388.
8. A. Saha, S. Ghosh, R. B. Weisman and A. A. Martí, *ACS Nano*, 2012, **6**, 5727-5734.
9. R. Jackson, B. Domercq, R. Jain, B. Kippelen and S. Graham, *Advanced Functional Materials*, 2008, **18**, 2548-2554.
10. B. B. Parekh, G. Fanchini, G. Eda and M. Chhowalla, *Applied Physics Letters*, 2007, **90**, 121913.
11. S. Paul, Y. S. Kang, Y.-K. Sun and D.-W. Kim, *Carbon*, 2010, **48**, 2646-2649.
12. S. Paul and D.-W. Kim, *Carbon*, 2009, **47**, 2436-2441.
13. J. Gao, X. Mu, X.-Y. Li, W.-Y. Wang, Y. Meng, X.-B. Xu, L.-T. Chen, L.-J. Cui, X. Wu and H.-Z. Geng, *Nanotechnology*, 2013, **24**, 435201.
14. M. H. A. Ng, T. H. Lysia, T. Huiwen and C. H. P. Poa, *Nanotechnology*, 2008, **19**, 205703.
15. H.-Z. Geng, K. K. Kim, K. P. So, Y. S. Lee, Y. Chang and Y. H. Lee, *Journal of the American Chemical Society*, 2007, **129**, 7758-7759.
16. S. Park, M. Vosguerichian and Z. Bao, *Nanoscale*, 2013, **5**, 1727-1752.
17. Z. Wu, Z. Chen, X. Du, J. M. Logan, J. Sippel, M. Nikolou, K. Kamaras, J. R. Reynolds, D. B. Tanner, A. F. Hebard and A. G. Rinzler, *Science*, 2004, **305**, 1273-1276.
18. S. J. Tans, A. R. M. Verschueren and C. Dekker, *Nature*, 1998, **393**, 49-52.
19. T. Dürkop, S. A. Getty, E. Cobas and M. S. Fuhrer, *Nano Letters*, 2003, **4**, 35-39.
20. R. Gao, Z. Pan and Z. L. Wang, *Applied Physics Letters*, 2001, **78**, 1757-1759.
21. D. R. Kauffman and A. Star, *Chemical Society Reviews*, 2008, **37**, 1197-1206.
22. F. Cicoira and C. Santato, *Advanced Functional Materials*, 2007, **17**, 3421-3434.
23. B. R. Lee, J. S. Kim, Y. S. Nam, H. J. Jeong, S. Y. Jeong, G.-W. Lee, J. T. Han and M. H. Song, *Journal of Materials Chemistry*, 2012, **22**, 21481-21486.
24. C. Hu and S. Hu, *J. Sens.*, 2009, 1-40.
25. B. L. Allen, P. D. Kichambare and A. Star, *Advanced Materials*, 2007, **19**, 1439-1451.
26. T. Kurkina, A. Vlandas, A. Ahmad, K. Kern and K. Balasubramanian, *Angewandte Chemie International Edition*, 2011, **50**, 3710-3714.
27. J. W. Kang and H. J. Hwang, *Carbon*, 2004, **42**, 3018-3021.
28. J. Y. Son, S. Ryu, Y.-C. Park, Y.-T. Lim, Y.-S. Shin, Y.-H. Shin and H. M. Jang, *ACS Nano*, 2010, **4**, 7315-7320.
29. H.-Z. Geng, K. K. Kim, C. Song, N. T. Xuyen, S. M. Kim, K. A. Park, D. S. Lee, K. H. An, Y. S. Lee, Y. Chang, Y. J. Lee, J. Y. Choi, A. Benayad and Y. H. Lee, *Journal of Materials Chemistry*, 2008, **18**, 1261-1266.
30. K. K. Kim, S.-M. Yoon, H. K. Park, H.-J. Shin, S. M. Kim, J. J. Bae, Y. Cui, J. M. Kim, J.-Y. Choi and Y. H. Lee, *New Journal of Chemistry*, 2010, **34**, 2183-2188.
31. J. T. Han, J. S. Kim, H. D. Jeong, H. J. Jeong, S. Y. Jeong and G.-W. Lee, *Journal of Materials Chemistry*, 2010, **20**, 8557-8562.
32. O. A. Barsan, G. G. Hoffmann, L. G. J. van der Ven and G. de With, *Faraday Discussions*, 2014, **173**, 365-377.
33. M. Zhang, S. Fang, A. A. Zakhidov, S. B. Lee, A. E. Aliev, C. D. Williams, K. R. Atkinson and R. H. Baughman, *Science*, 2005, **309**, 1215-1219.
34. C. Niu, *MRS Bull.*, 2011, **36**, 766-773.
35. B.-S. Kim, D. Kim, K.-W. Kim, T. Lee, S. Kim, K. Shin, S. Chun, J. H. Han, Y. S. Lee and H.-j. Paik, *Carbon*, 2014, **72**, 57-65.
36. D. Jung, K. H. Lee, D. Kim, D. Burk, L. J. Overzet and G. S. Lee, *Japanese Journal of Applied Physics*, 2013, **52**, 03BC03.
37. S. Roth and H. J. Park, *Chemical Society Reviews*, 2010, **39**, 2477-2483.
38. V. M. F. L. De, S. H. Tawfick, R. H. Baughman and A. J. Hart, *Science*, 2013, **339**, 535-539.
39. K. Balasubramanian and M. Burghard, *Small*, 2005, **1**, 180-192.
40. P. Bilalis, D. Katsigiannopoulos, A. Avgeropoulos and G. Sakellariou, *RSC Advances*, 2014, **4**, 2911-2934.
41. P. Li, H. Liu, Y. Ding, Y. Wang, Y. Chen, Y. Zhou, Y. Tang, H. Wei, C. Cai and T. Lu, *Journal of Materials Chemistry*, 2012, **22**, 15370-15378.
42. Y. Y. Huang and E. M. Terentjev, *Polymers*, 2012, **4**, 275-295.
43. A. Lucas, C. Zakri, M. Maugey, M. Pasquali, P. v. d. Schoot and P. Poulin, *The Journal of Physical Chemistry C*, 2009, **113**, 20599-20605.
44. P. Vichchulada, M. A. Cauble, E. A. Abdi, E. I. Obi, Q. Zhang and M. D. Lay, *The Journal of Physical Chemistry C*, 2010, **114**, 12490-12495.
45. S. Luo, T. Liu, S. M. Benjamin and J. S. Brooks, *Langmuir*, 2013, **29**, 8694-8702.
46. S. Mouri, Y. Miyauchi and K. Matsuda, *The Journal of Physical Chemistry C*, 2012, **116**, 10282-10286.
47. J. I. Paredes and M. Burghard, *Langmuir*, 2004, **20**, 5149-5152.
48. S. Pfeifer, S.-H. Park and P. R. Bandaru, *Journal of Applied Physics*, 2010, **108**, -.
49. C. Y. Hu, Y. J. Xu, S. W. Duo, R. F. Zhang and M. S. Li, *Journal of the Chinese Chemical Society*, 2009, **56**, 234-239.
50. K. Matyjaszewski, T. E. Patten and J. Xia, *J. Am. Chem. Soc.*, 1997, **119**, 674-680.
51. A. Yu, E. Bekyarova, M. E. Itkis, D. Fakhrutdinov, R. Webster and R. C. Haddon, *Journal of the American Chemical Society*, 2006, **128**, 9902-9908.
52. S. N. Barman, M. C. LeMieux, J. Baek, R. Rivera and Z. Bao, *ACS Applied Materials & Interfaces*, 2010, **2**, 2672-2678.
53. D. Hecht, L. Hu and G. Grüner, *Applied Physics Letters*, 2006, **89**, 1-3.
54. F. Mirri, A. W. K. Ma, T. T. Hsu, N. Behabtu, S. L. Eichmann, C. C. Young, D. E. Tsentalovich and M. Pasquali, *ACS Nano*, 2012, **6**, 9737-9744.
55. S. L. Hellstrom, H. W. Lee and Z. Bao, *ACS Nano*, 2009, **3**, 1423-1430.
56. R. S. Lee, H. J. Kim, J. E. Fischer, A. Thess and R. E. Smalley, *Nature*, 1997, **388**, 255-257.
57. M. S. Dresselhaus, G. Dresselhaus, R. Saito and A. Jorio, *Physics Reports*, 2005, **409**, 47-99.
58. I. O. Maciel, N. Anderson, M. A. Pimenta, A. Hartschuh, H. Qian, M. Terrones, H. Terrones, J. Campos-Delgado, A. M. Rao, L. Novotny and A. Jorio, *Nat Mater*, 2008, **7**, 878-883.

Figure list

Figure 1. ^{1}H NMR spectrum of (a) furfuryl alcohol and (b) furfuryl methacrylate. The symbols (*) indicate solvent signal.

Figure 2. ^{1}H NMR spectra of *p*(FMA-*co*-DMAEMA) with molar composition 70:30 (FMA:DMAEMA). The symbols (*) indicate solvent signal.

Figure 3. Transmittance changes in the SWCNT dispersions over the course of 3 days. Average transmittance changes are 21.2 (with dispersant 1), 1.39 (with 2), 0.10 (with 3), 55.0 (with 4) and 4.98 (with 5).

Figure 4. (a) TEM images of exfoliated SWCNTs with *p*(FMA-*co*-DMAEMA) and (b) length distribution of dispersed SWCNTs.

Figure 5. AFM images of individually dispersed SWCNTs, (a) low magnification, (b) high magnification image of the SWCNTs and (c) indicate height profile about being shown in (b).

Figure 6. Sheet resistance versus transmittance at 550 nm (a) before and after treatment with previously reported values for comparison

Figure 7. FE-SEM images of (a) the SWCNT network deposited on PET substrate and (b) the SWCNT network after chemical treatment with HNO_3 and $SOCl_2$.

Figure 8. (a) Raman spectra of pristine SWCNT, an untreated SWCNT-based TCF, and chemically treated TCFs. (b) I_D/I_G versus $I_{G'}/I_G$ for pristine SWCNT, an untreated SWCNT-based TCF, and chemically treated TCFs.

Figure 9. The change in sheet resistance (R_s / $R_{s,0}$) of a SWCNT TCF with repeated bending cycles. The initial sheet resistance ($R_{s,0}$) was 85.75 Ω/□.

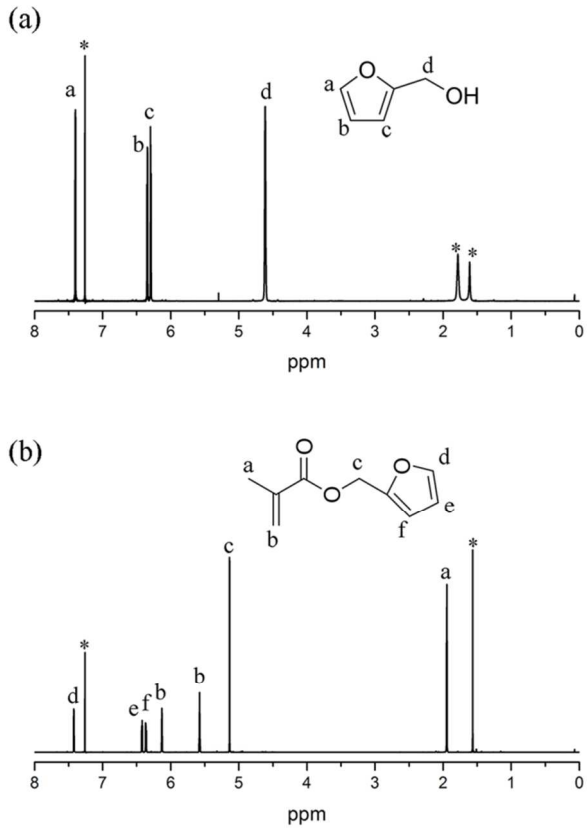

Figure 1. ^{1}H NMR spectrum of (a) furfuryl alcohol and (b) furfuryl methacrylate. The symbols (*) indicate solvent signal.

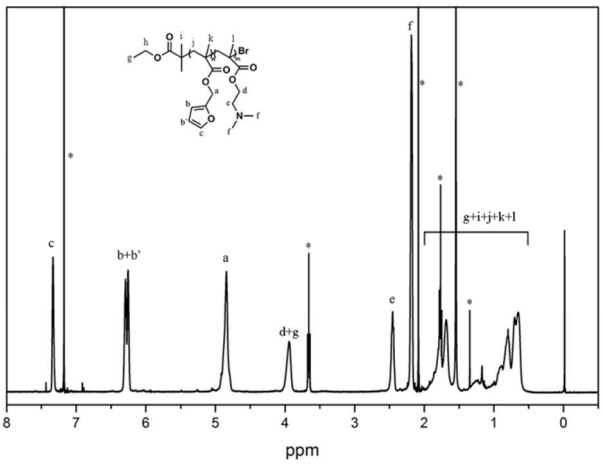

Figure 2. ^{1}H NMR spectra of *p*(FMA-*co*-DMAEMA) with molar composition 70:30 (FMA:DMAEMA). The symbols (*) indicate solvent signal.

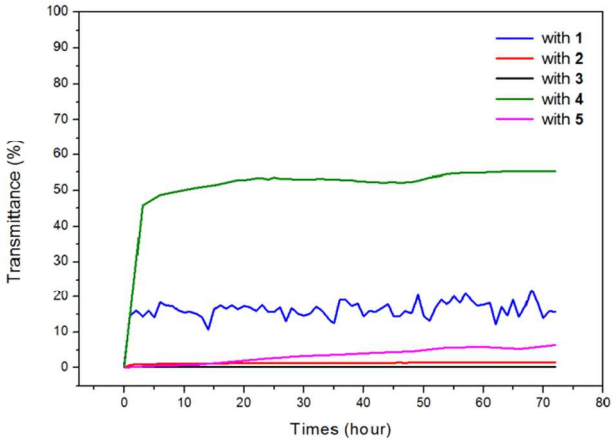

Figure 3. Transmittance changes in the SWCNT dispersions over the course of 3 days. Average transmittance changes are 21.2 (with dispersant 1), 1.39 (with 2), 0.10 (with 3), 55.0 (with 4) and 4.98 (with 5).

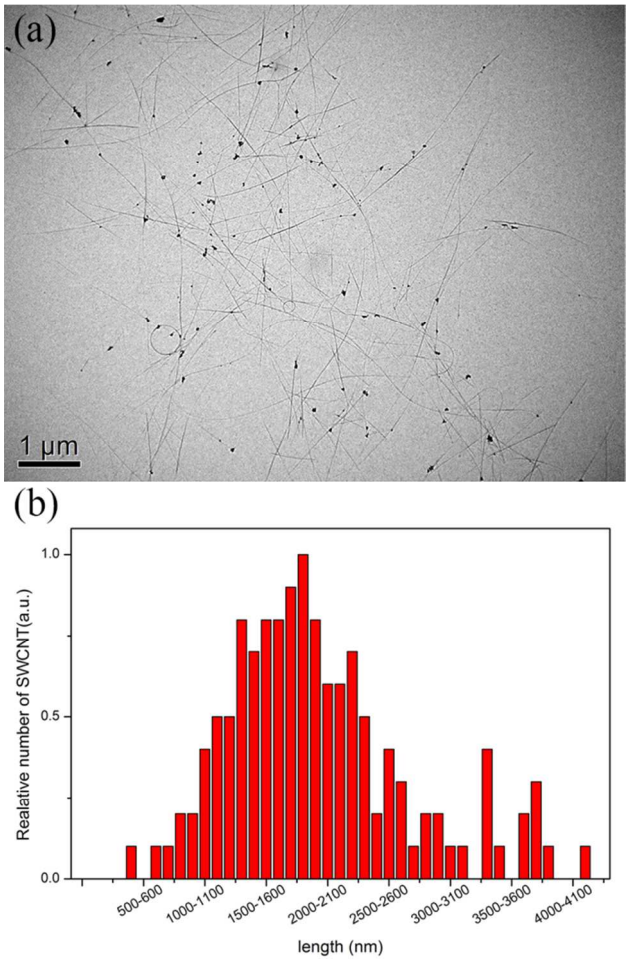

Figure 4. (a) TEM images of exfoliated SWCNTs with *p*(FMA-*co*-DMAEMA) and (b) length distribution of dispersed SWCNTs.

(Double column)

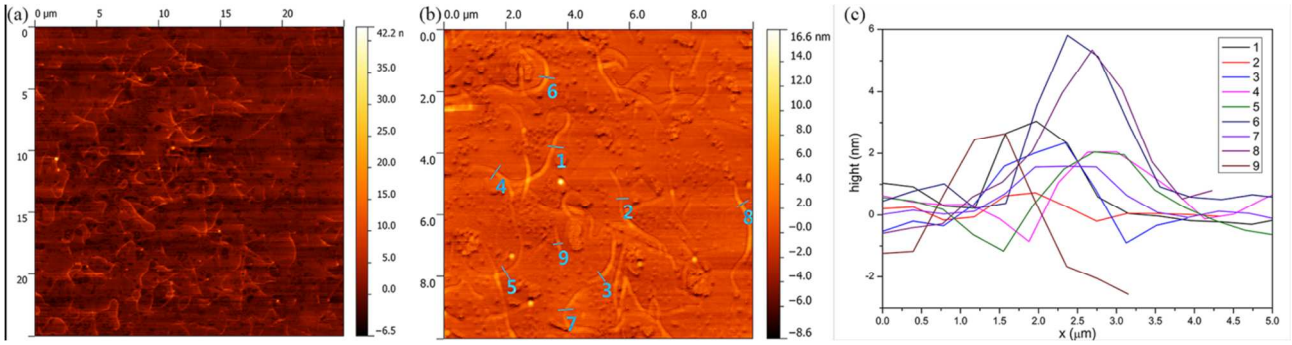

Figure 5. AFM images of individually dispersed SWCNTs, (a) low magnification, (b) high magnification image of the SWCNTs and (c) indicate height profile about being shown in (b).

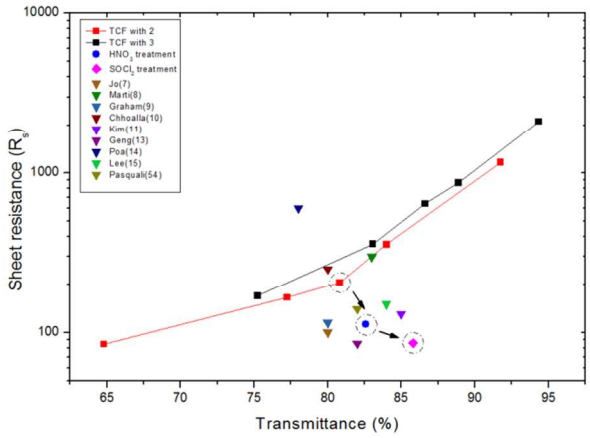

Figure 6. Sheet resistance versus transmittance at 550 nm before and after treatment with previously reported values for comparison.

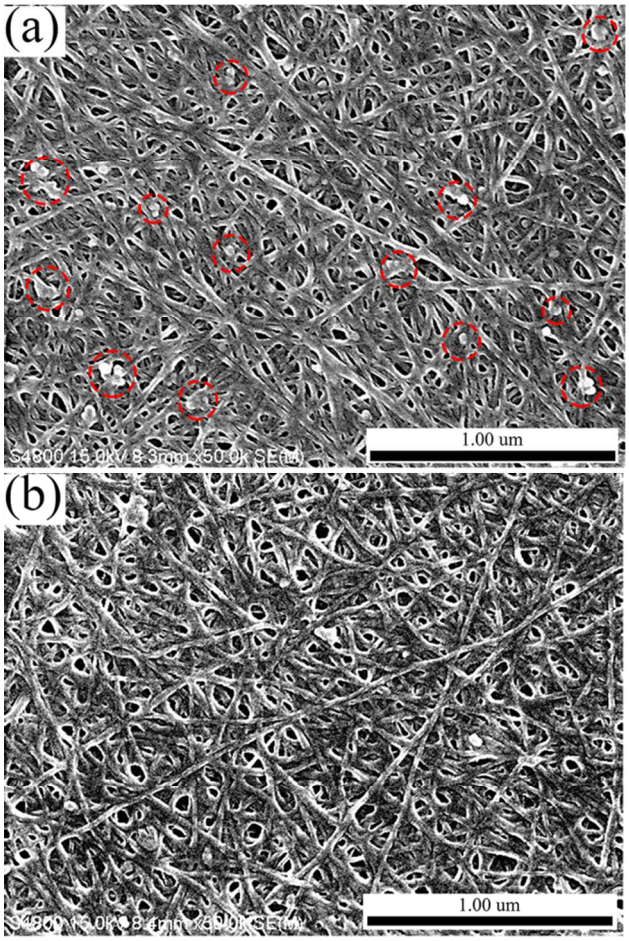

Figure 7. FE-SEM images of (a) the SWCNT network deposited on PET substrate and (b) the SWCNT network after chemical treatment with HNO_3 and $SOCl_2$.

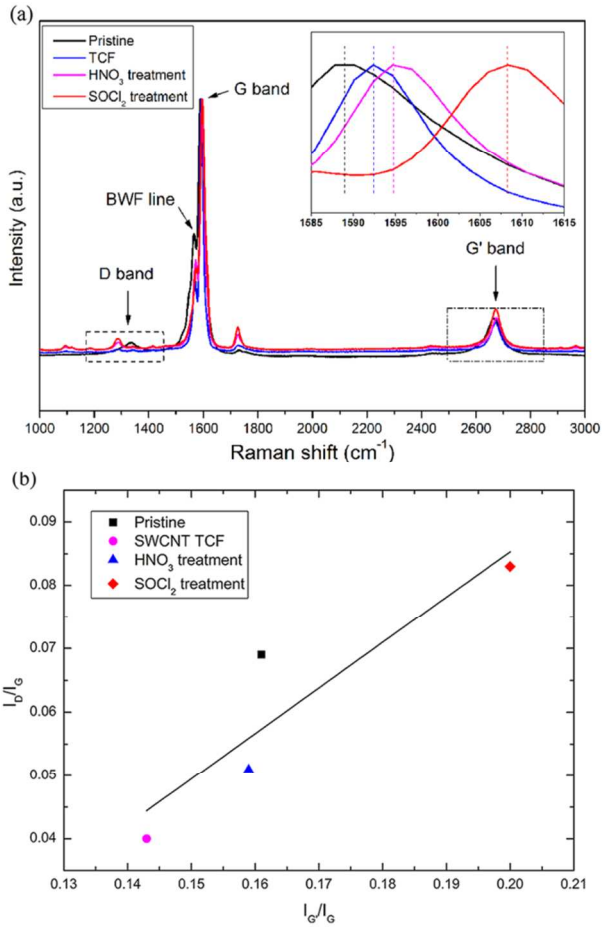

Figure 8. (a) Raman spectra of pristine SWCNT, an untreated SWCNT-based TCF, and chemically treated TCFs. (b) I_D/I_G versus $I_{G'}/I_G$ for pristine SWCNT, an untreated SWCNT-based TCF, and chemically treated TCFs.

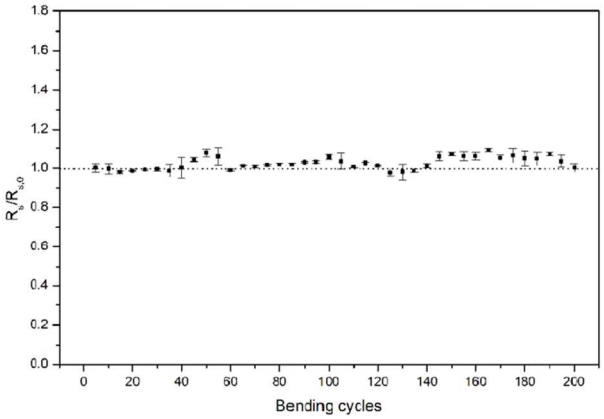

Figure 9. The change in sheet resistance (R_s / $R_{s,0}$) of a SWCNT TCF with repeated bending cycles. The initial sheet resistance ($R_{s,0}$) was 85.75 Ω/□.

Scheme list

Scheme 1. Synthesis of polymeric dispersant by ATRP, *p*(DMAEMA-*co*-FMA).

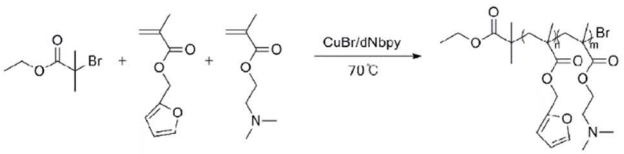

Scheme 1. Synthesis of polymeric dispersant by ATRP, *p*(DMAEMA-*co*-FMA).

Table list

(Double column)

Table 1. Molecular weight and composition data for polymeric dispersants

	$[EBiB]_0 : [FMA]_0 : [DMAEMA]_0$	Conversion of FMA[a] (%)	Conversion of DMAEMA[a] (%)	Molecular weight ($M_{n,theory}$)[b]	Molecular weight (M_n)[c]	M_w/M_n[c]	Composition (FMA : DMAEMA)[d]
1	1 : 150 : 0	71.1	-	17,900	18,400	1.44	100 : 0
2	1 : 105 : 45	60.8	55.0	14,600	17,900	1.45	69.2: 30.8
3	1 : 75 : 75	60.0	56.4	14,000	16,000	1.33	50.8 : 49.2
4	1 : 45 : 105	52.8	54.4	13,000	14,000	1.50	30.7 : 69.3
5	1 : 0 : 150	-	53.3	12,700	13,800	1.17	0 : 100

[a] Monomer conversion were determined by gas chromatography (GC)
[b] Theoretical molecular weight was calculated from conversion.
$(MW_{EBiB}+[FMA]_0/[EBiB]_0\times conversion\times MW_{FMA}+[DMAEMA]_0/[EBiB]_0\times conversion\times MW_{DMAEMA})$
[c] Molecular weight data were obtained by gel permeation chromatography (GPC).
[d] Composition of monomer unit in polymer were determined by ^{1}H NMR

Table 2. FOM values of TCF by each treatment

	T [%]	R_s [Ω/□]	FOM[a)]
As coated	80	210	7.6
HNO_3	82	112	16.1
$SOCl_2$	85	85.75	26.0

[a)]FOM values were calculated using Equation (1)

Table 3. Raman data associated defect of SWCNTs and as-prepared and chemically treated SWCNT films

Sample	$I_{G'}/I_G$	I_D/I_G	Defect [%]
Pristine SWCNT	0.161	0.069	6.9%
SWCNT TCF	0.143	0.040	4.0%
HNO_3 treatment	0.159	0.051	5.1%
$SOCl_2$ treatment	0.200	0.083	8.3%